Memorias del 2023 Congreso Nacional de Control Automático
25-27 de Octubre, 2023. Acapulco, Guerrero, México.

Cyber-physical Multi-robot Formation: Virtual Agents Approach and Low-Cost Experiments ⋆

Huber Giron-Nieto * **Oliver Ochoa-García** *
Eduardo Gamaliel Hernandez-Martinez **
Mario Ramírez-Neria ** **Guillermo Fernandez-Anaya** ***
Enrique D. Ferreira-Vazquez **** **Jose Job Flores-Godoy** †

* *Department of Science and engineering, Universidad Iberoamericana Puebla, 072820 Puebla, México. (e-mail: huber.giron2@iberopuebla.mx, oliver.ochoa2@iberopuebla.mx).*
** *Institute of Applied Research and Technology, Universidad Iberoamericana Ciudad de México, 01219, Mexico City, Mexico. (e-mail: eduardo.gamaliel@ibero.mx, mario.ramirez@ibero.mx)*
*** *Physics and Math Department, Universidad Iberoamericana Ciudad de México, 01219, Mexico City, Mexico. (e-mail: guillermo.fernandez@ibero.mx)*
**** *Engineering Department, Universidad Católica del Uruguay, Montevideo 11600, Uruguay. (enrique.ferreira@ucu.edu.uy)*
† *Exact and Natural Sciences Department, Universidad Católica del Uruguay, Montevideo 11600, Uruguay. (jose.flores@ucu.edu.uy)*

Abstract: A cyber-physical formation includes all the strategies to coordinate mobile robots moving in different physical workspaces sharing information through internet and the cloud. This work addresses a formation scheme of robots moving in two different workspaces. The control strategy is based on virtual agents used like "avatars" which must converge to the position of the robots in the opposite workspace. The control approach is designed for robots modeled as single integrators and extended to the case of unicycle-type robots. Results of numerical simulations and real experiments are shown using a low-cost cyber-physical micro-robot platform based on a camera as position and orientation sensor.

Keywords: Cyber-physical, formation control, mobile robots, unicycles, multi-agent systems.

1. INTRODUCTION

The motion coordination of multiple mobile robots is an important theoretical and technological research area in the industrial and service fields (Canudas de Wit et al., 1996; Valentim et al., 2019). Groups of robots have been widely used for logistics (Hernandez-Martinez et al., 2014), the transportation of large objects (Farrugia and Fabri, 2018) surveillance and perimeter vigilance (Mantha et al., 2020), among others. The main contributions have been addressed for differential-drive or unicycle-type wheeled robots (González-Sierra et al., 2013), omnidirectional robots (Hernandez-Martinez et al., 2013) and car-like configurations. The basic group coordination problems are: formation control (Ferreira-Vazquez et al., 2016), the formation tracking or marching control (Oh et al., 2015), and the inter-robot collision avoidance (Lopez-Gonzalez et al., 2016).

The fourth industrial revolution, known as Industry 4.0, incorporates new enabling technologies for a better communicated world, as in Gallo et al. (2021). Wireless communication devices with high-bandwidth, the use of the cloud for data storage and analysis and the embedded computing architectures promote new opportunities for an enhanced distributed motion coordination of mobile robots. Thus, the robots can achieve coordinated motion across different and remote workspaces. Besides, the formation control laws could be executed onboard the robots themselves or in the cloud. Therefore, the group coordination becomes a cyber-physical setup with decentralized real hardware working online with the internet and the cloud, Escobar et al. (2020).

⋆ The authors acknow the financial support from Universidad Iberoamericana Puebla through the Institute Design and Technological Innovation (IDIT), and from Universidad Iberoamericana Ciudad de México through the project fund DINVP-0051.

The cyber-physical formation schemes are a recent focus for the multi-robot control community. Recent advances are shown in Lian et al. (2021), Pikner et al. (2021), Kruglova et al. (2019). The formation problem across different workspaces, sharing information through the internet, generates new challenges for the control schemes. Kim et al. (2008) have studied the effect of delays in the internet communication, Lo et al. (2003) the problem of communication losses between workspaces and Shahzad and Roth (2016) for the intermittence in the internet links.

Recently, some robotics platforms have been built for the experimentation of cyber-physical formation approaches. For example in Escobar et al. (2020), a multi-robot platform is designed for educational purposes with cyber-physical features using omnidirectional mobile robots and MQTT protocol. Thus, the study of cyber-physical behaviors in multi-robot systems requires a flexible platform that enables monitoring and control of the multi-workspace setup.

This work is a first stage for the modeling, control and experimentation of cyber-physical formations of mobile robots. The main contributions are highlighted by the next points:

- The design and implementation of a control strategy for a cyber-physical formation of mobile robot systems moving in two workspaces.
- The control approach is based on the use of virtual agents which converge to the physical robots moving in the opposite workspace. The convergence is analyzed for the general case of n robots. Under this control scheme the robots behave as if they move in a unique workspace.
- The control approach is developed for 2D single integrator robots, but it is extended to unicycle-type robots with two wheels and it is validated by numerical simulations.
- Finally, a novel low cost experimental platform is built. An experiment is shown using four robots in two different physical spaces communicated through an internet connection with a MQTT protocol.

The paper is organized as follows. The problem definition is given in Section 2. The control strategy is presented in the Section 3. Numerical simulations are shown in Section 4. The experimental platform and results are shown in Section 5. Finally, some concluding remarks are proposed in Section 6.

2. PROBLEM FORMULATION

In this section, the cyber-physical formation problem is defined for n point-robots moving in two different workspaces.

Let $\mathscr{R} = \{R_1, ..., R_n\}$ be a set of mobile robots. Consider that these n robots move in two different workspaces $\mathscr{W}_1$ and $\mathscr{W}_2$. Without loss of generality, consider that

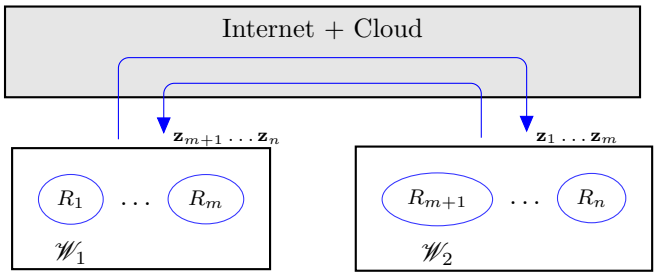

Fig. 1. Communication between workspaces $\mathscr{W}_1$ and $\mathscr{W}_2$.

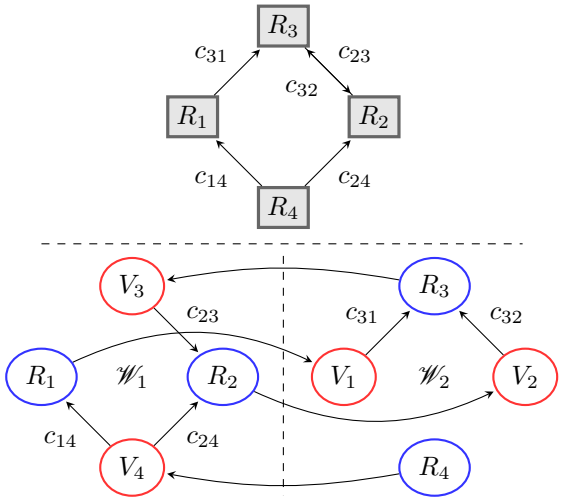

Fig. 2. Example of the relationship between the original formation graph $\mathscr{G}$ (above) and workspaces $\mathscr{W}_1$ and $\mathscr{W}_2$ and combined graph $\hat{\mathscr{G}}$ (below).

$\mathscr{R}_1 = \{R_1, ..., R_m\}$, with $1 < m < n$ is the subset of robots moving in $\mathscr{W}_1$ and $\mathscr{R}_2 = \{R_{m+1}, ..., R_n\}$ is the subset of robots moving in $\mathscr{W}_2$. Therefore $\mathscr{R} = \mathscr{R}_1 \cup \mathscr{R}_2$ with $\mathscr{R}_1 \cap \mathscr{R}_2 = \emptyset$. Define $\mathbf{z}_i = [x_i, y_i]^\top \in \mathbb{R}^2$ as the 2D position of R_i in $\mathscr{W}_1$ or $\mathscr{W}_2$.

The main goal of this work is to construct a formation control strategy such that the robots in the two workspaces converge to a global formation as if they were in the same space. To do this, the information about the positions $\mathbf{z}_i$, $i = 1, ..., n$ must be shared between $\mathscr{W}_1$ and $\mathscr{W}_2$ as illustrated in Fig. 1 using internet and the cloud. Let us assume a desired global formation graph $\mathscr{G}$ for n robots is defined by an adjacency matrix $\mathbf{A}$, a set of relative positions $\mathscr{C}$ and a Laplacian matrix $\mathbf{L}$. The challenge in a cyber-physical configuration is to converge to the formation $\mathscr{G}$ with the absence of certain robots in each workspace. This paper proposes the use of virtual robots. Thus, for each $R_i \in \mathscr{R}_1$, $i = 1, ..., m$ define a virtual robot $V_i \in \mathscr{V}_2$, $i = 1, ..., m$ and for each $R_i \in \mathscr{R}_2$, $i = m+1, ..., n$ define a virtual robot $V_i \in \mathscr{V}_1$, $i = m+1, ..., n$. Thus, there are also n virtual robots divided in $\mathscr{V}_1$ and $\mathscr{V}_2$. Let $\mathbf{v}_i \in \mathbb{R}^2$ be the 2D position of each virtual robot V_i. Finally, $\mathscr{W}_i = \mathscr{R}_i \cup \mathscr{V}_i, i = 1, 2$.

Consider that both, the real and virtual robots are modeled as single integrators as follows:

$$\begin{aligned}\dot{\mathbf{z}}_i &= \mathbf{u}_i, \qquad i = 1, ..., n \\ \dot{\mathbf{v}}_i &= \mathbf{w}_i, \qquad i = 1, ..., n\end{aligned} \tag{1}$$

where $\mathbf{u}_i \in \mathbb{R}^2$ and $\mathbf{w}_i \in \mathbb{R}^2$ are the control inputs for the real and virtual robots, respectively.

For all robots in any workspace $\mathscr{W}_i$ a new formation graph $\hat{\mathscr{G}}$ is derived from $\mathscr{G}$ as follows. For each $R_j \in \mathscr{R}_i$ let $\mathscr{N}_{ij}^R$ and $\mathscr{N}_{ij}^V$ be the adjacent subsets of indexes of the real and virtual robots in $\mathscr{W}_i$ who are communicated to R_j according to the following:

$$\begin{aligned}\mathscr{N}_{ij}^R &= \{k | \mathbf{A}_{jk} \neq 0, \quad R_j, R_k \in \mathscr{R}_i\} \\ \mathscr{N}_{ij}^V &= \{k | \mathbf{A}_{jk} \neq 0, \, R_j \in \mathscr{R}_i, V_k \in \mathscr{V}_i\}\end{aligned} \tag{2}$$

Besides, all virtual robots V_j are communicated only to their real counterpart R_j located in the other workspace W_{3-i}. An example of the communication topology is shown in Fig. 2. On the other side, for each $(j,k)|k \in \mathscr{N}_{ij}^R \cup \mathscr{N}_{ij}^V$ let $\mathbf{c}_{kj}$ define the static and predefined desired relative position vector $\mathbf{c}_{kj} \in \mathbb{R}^2, \mathbf{c}_{kj} \in \mathscr{C}$. By design, it is straightforward to show that if $\mathscr{G}$ has a directed spanning tree then $\hat{\mathscr{G}}$ also has one. Having a directed spanning tree, it is well-known that the laplacian matrix of $\mathscr{G}$ and $\hat{\mathscr{G}}$ given by $\mathbf{L}$ and $\hat{\mathbf{L}}$ respectively, have the eigenvalue set $E = \{\lambda_1, ..., \lambda_n\}$ with $\lambda_1 = 0$ and $\lambda_i > 0$, $i = 2, ..., n$ (Olfati-Saber, 2007).

3. CONTROL STRATEGY

The control strategy needs to have at least a leader robot. Let us define $R_n \in \mathscr{W}_2$ as the leader robot, and $\mathbf{z}_d, \dot{\mathbf{z}}_d \in \mathbb{R}^2$ and as the desired position and velocity of the trajectory for the leader. The control strategy for the virtual robots $V_j \in \mathscr{W}_i$ is designed to track its corresponding real robot R_j that belongs to the other workspace $\mathscr{W}_{3-i}$, according to the following law:

$$\mathbf{w}_j = k_v(\mathbf{z}_j - \mathbf{v}_j) + \dot{\mathbf{z}}_d, \quad k_v > 0, \, j = 1, \ldots, n. \tag{3}$$

with $k_v > 0$ the control gain for the virtual robots. The control law for the real robots R_j is given by the following:

$$\begin{aligned}\mathbf{u}_j = & k_r \sum_{k \in \cup_i \mathscr{N}_{ij}^R} (\mathbf{z}_k + \mathbf{c}_{kj} - \mathbf{z}_j) + \cdots \\ & k_r \sum_{k \in \cup_i \mathscr{N}_{ij}^V} (\mathbf{v}_k + \mathbf{c}_{kj} - \mathbf{z}_j) + \dot{\mathbf{z}}_d,\end{aligned} \tag{4}$$

with $k_r > 0$ the control gain for the real robots and $j = 1, \ldots, n-1$. The control strategy for the leader robot R_n is given by

$$\begin{aligned}\mathbf{u}_n = & k_r \sum_{k \in \mathscr{N}_{2n}^R} (\mathbf{z}_k + \mathbf{c}_{kn} - \mathbf{z}_n) + \ldots \\ & k_r \sum_{k \in \mathscr{N}_{2n}^V} (\mathbf{v}_k + \mathbf{c}_{kn} - \mathbf{z}_n) + k_c(\mathbf{z}_d - \mathbf{z}_n) + \dot{\mathbf{z}}_d.\end{aligned} \tag{5}$$

Defining the relative positions of the robots with respect to the desired trajectory $\tilde{\mathbf{z}}_j = \mathbf{z}_j - \mathbf{z}_d$ and $\tilde{\mathbf{v}}_j = \mathbf{v}_j - \mathbf{z}_d$, equations (3),(4) and (5) have a relative consensus defined by

$$\begin{aligned}\tilde{\mathbf{v}}_j^\star = & \tilde{\mathbf{z}}_j^\star, \; \forall j \\ 0 = & \sum_{k \in \cup_i \mathscr{N}_{ij}^R} (\tilde{\mathbf{z}}_k^\star + \mathbf{c}_{kj} - \tilde{\mathbf{z}}_j^\star) + \ldots \\ & \sum_{k \in \cup_i \mathscr{N}_{ij}^V} (\tilde{\mathbf{v}}_k^\star + \mathbf{c}_{kj} - \tilde{\mathbf{z}}_j^\star) \qquad \forall j < n \\ \tilde{\mathbf{z}}_n^\star = & 0.\end{aligned} \tag{6}$$

Let $e_j^R = \tilde{\mathbf{z}}_j - \tilde{\mathbf{z}}_j^\star$ and $e_j^V = \tilde{\mathbf{v}}_j - \tilde{\mathbf{v}}_j^\star$ be the relative error with respect to the consensus trajectory of the real and virtual robots respectively. Using the above equations, the error dynamics can be expressed as

$$\begin{bmatrix}\dot{\mathbf{e}}^V \\ \dot{\mathbf{e}}^R\end{bmatrix} = \left(\begin{bmatrix} -k_v \mathbf{I}_n & k_v \mathbf{I}_n \\ k_r \mathbf{E}_{21} & k_r \mathbf{E}_{22} + k_c \mathbf{q}_n \mathbf{q}_n^\top \end{bmatrix} \otimes \mathbf{I}_2 \right) \begin{bmatrix}\mathbf{e}^V \\ \mathbf{e}^R\end{bmatrix} \tag{7}$$

where

$$\mathbf{e}^V = [e_1^{V\top} \ldots e_n^{V\top}]^\top \tag{8}$$

$$\mathbf{e}^R = [e_1^{R\top} \ldots e_n^{R\top}]^\top \tag{9}$$

$$\mathbf{E}_{21} + \mathbf{E}_{22} = -\mathbf{L} \tag{10}$$

$$\mathbf{q}_n = [\mathbf{0}_{n-1}^\top \, 1]^\top. \tag{11}$$

with $\mathbf{0}_{n-1}$ a zero vector with dimension $n-1$.

Using the fact that the communication topology is given by $\hat{\mathscr{G}}$, it can be shown that the system dynamics (7) converges to the origin, achieving relative consensus given by equations (6). A Gershgorin disk-based proof is omitted here for reasons of space.

4. NUMERICAL SIMULATION

The numerical simulation was programmed in Matlab-Simulink©$R2022b$ with a variable-step continuous implicit solver.

Fig. 3 shows the numerical simulation of the control approach with $n = 4$, and $m = 2$, i.e. the total set of robots is $\mathscr{R} = \{R_1, R_2, R_3, R_4\}$, where $\mathscr{R}_1 = \{R_1, R_2\} \in \mathscr{W}_1$ and $\mathscr{R}_2 = \{R_3, R_4\} \in \mathscr{W}_2$ as shown in Fig. 3a. The leader robot is R_4. Therefore $\mathscr{V}_1 = \{V_3, V_4\}$ and $\mathscr{V}_2 = \{V_1, V_2\}$, and the total members of each workspace are $\mathscr{W}_1 = \{R_1, R_2, V_3, V_4\}$ and $\mathscr{W}_2 = \{V_1, V_2, R_3, R_4\}$.

The adjacent subsets for the real robots are defined as $\mathscr{N}_{11}^R = \emptyset$, $\mathscr{N}_{11}^V = \{V_3, V_4\}$, $\mathscr{N}_{12}^R = \emptyset$, $\mathscr{N}_{12}^V = \{V_3, V_4\}$, $\mathscr{N}_{23}^R = \emptyset$, $\mathscr{N}_{23}^V = \{V_1, V_2\}$, $\mathscr{N}_{24}^R = \emptyset$, $\mathscr{N}_{24}^V = \{V_1, V_2\}$ as shown in Fig. 3a. The desired final posture of the robots is a diamond-shaped formation, as if all 4 real robots would be in the same workspace. To achieve this desired formation pattern, the relative vectors are given by $c_{13} = [a, b]^\top$, $c_{14} = [a, -b]^\top$, $c_{23} = [-a, b]^\top$, $c_{24} = [-a, -b]^\top$, with $a = 280$, $b = 140$ and by construction $c_{31} = -c_{13}$, $c_{41} = -c_{14}$, $c_{32} = -c_{23}$ and $c_{42} = -c_{24}$.

Fig. 3b shows the trajectories of the real and virtual robots using the control law (3)-(4)-(5) with $k_v = 100$,

$k_r = 100$, $k_c = 100$ and the desired trajectory of the leader robot R_4 given by $\mathbf{z}_d = [72\cos t, 84 + 72\sin t]^\top$. Note that the robots converge to the desired formation pattern which is observed by the errors´ convergence shown in the Fig. 3c. Finally, the control inputs are depicted in the Fig. 3d.

5. EXPERIMENTAL WORK

5.1 Experimental platform

The control approach was proved in a novel low-cost experimental robotics platform composed by the four mobile robots shown in Fig. 4. Each unicycle-type robots are integrated by two DC motors manufactured by Pololu© with plastic wheels, controlled by an Arduino pro-micro with Bluetooth wireless communicated to a PC. The case of the robots is made with 3D printer with an Aruco-Tag on the top.

The control implementation is based on the scheme presented in Fig. 5. The four robots are placed in two different workspaces. Every workspace has a Logitech© web camera model $C920$ with a resolution of 1280×720 pixels, installed to a height of 40 mm, that generates a viewed area of around 75 mm $\times$40 mm. Therefore, the resolution of every square pixel is about 0.36mm^2. Every camera is connected to an Intel© core $i7$ PC. The PC reads the Aruco tags at a sample rate of 0.1 s detecting the ID of the robots and calculating the position and orientation of every robot using the OpenCV visual processing toolbox. The positions and orientations of the robots are sent to the internet through a MQTT IoT protocol using a HIVEMQ© broker. The communication is bidirectional and the two workspaces are connected online. The control law is programmed in every PC using Phyton version 3.10 at the same sample rate of 0.1s, sending the control inputs to every robot using the Bluetooth wireless communication. Note that the control setup is low-cost and scalable. Also, the experimental setup is modular using commercial components allowing its expansion to more robots and workspaces. The use of the HIVEMQ© broker is free. Thus, this experimental setup becomes the base of a ad-hoc platform for proving future and more complex cyber-physical formation approaches.

5.2 Extension of the control to unicycle-type robots

The kinematic model of the unicycle-type robots shown in Fig. 4 is given, according to the Fig. 6, by

$$\dot{x}_i = v_i \cos\theta_i \tag{12}$$
$$\dot{y}_i = v_i \sin\theta_i \tag{13}$$
$$\dot{\theta}_i = w_i \tag{14}$$

with $i = 1, ..., n$, where $[x_i, y_i]^\top$ is the 2D coordinate of the robot and θ_i is its orientation angle with respect to the horizontal axis. The v_i and w_i are the longitudinal and rotational control inputs respect to the middle point

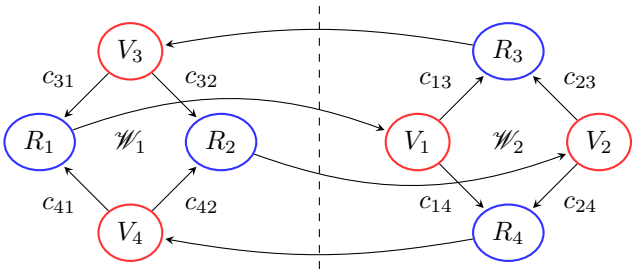

(a) Experimental workspaces and formation topology.

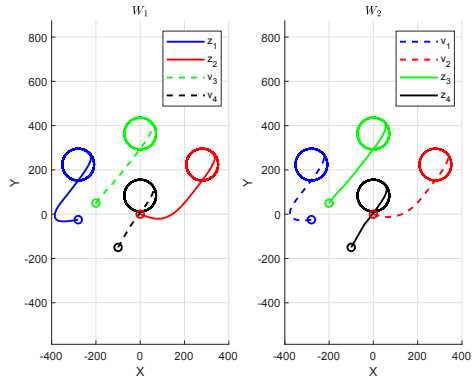

(b) Trajectories of robots.

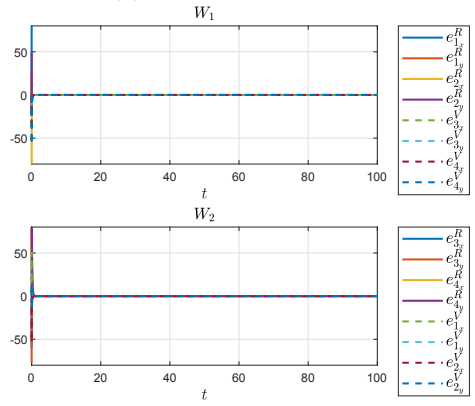

(c) Convergence of the errors.

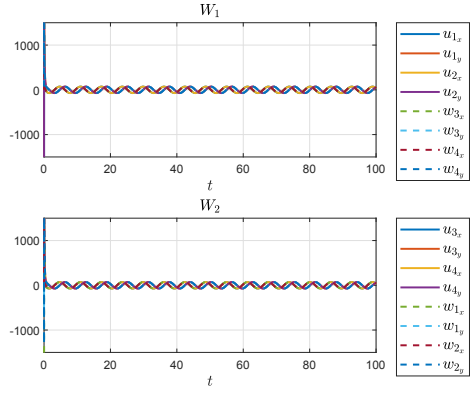

(d) Control inputs.

Fig. 3. Numerical simulation with $\mathscr{W}_1 = \{R_1, R_2, V_3, V_4\}$ and $\mathscr{W}_2 = \{V_1, V_2, R_3, R_4\}$.

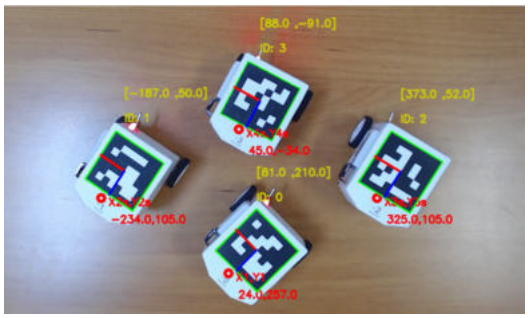

Fig. 4. Photo of the experimental robots.

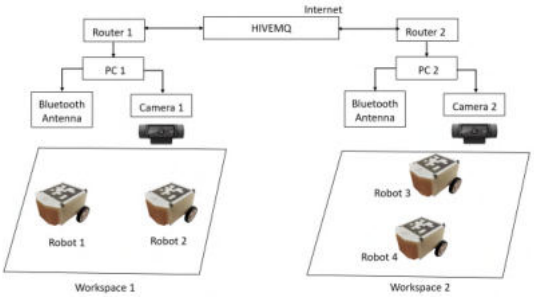

Fig. 5. Control implementation.

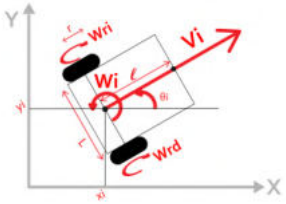

Fig. 6. Kinematic model of a unicycle-type robot.

of the axis' wheels. These two body-level velocities can be converted to the velocities of the wheels through

$$w_{R_i} = \frac{v_i}{r} + \frac{w_i L}{2r}, \qquad w_{L_i} = \frac{v_i}{r} - \frac{w_i L}{2r} \tag{15}$$

where w_{R_i} and w_{L_i} are the angular velocities of the right and left wheels, respectively, r is the radius of the wheels and L is the length is the distance between the wheels.

Choosing the frontal point as control output, shown in Fig. 6, with

$$\alpha_i = [x_i + \ell\cos\theta_i, y_i + \ell\sin\theta_i]^\top \tag{16}$$

where $\ell \neq 0$, its dynamics is given by

$$\dot{\alpha}_i = A_i(\theta_i)[v_i, w_i]^\top \tag{17}$$

where $A_i(\theta_i) = \begin{bmatrix} \cos\theta_i & -\ell\sin\theta_i \\ \sin\theta_i & \ell\cos\theta_i \end{bmatrix}$.

Since $\det A_i(\theta_i) = \ell \neq 0$, it is possible to linearize the dynamics of α_i using the control

$$[v_i, w_i]^\top = A_i^{-1}(\theta_i)\mathbf{u}_i \tag{18}$$

with $\mathbf{u}_i \in \mathbb{R}^2$ as an auxiliary control. Note that in the closed-loop control (17)-(18), the dynamics is reduced $\dot{\alpha}_i = \mathbf{u}_i$ and the nonlinearities are eliminated resulting in the single integrator given by (1). Therefore, the control approach can be extended to the unicycle-type robots using the control law (18) where $\mathbf{u}_i$ is defined by the equations (3), (4) and (5) but dependent on the coordinates α_i of the robots.

5.3 Experimental results

Fig. 7 shows the experimental results of the simulation case developed in section 4. The parameters of the robots are $r = 15$ mm, $\ell = 10$ mm and $L = 45$ mm. The control gains are given by $k_v = 100$, $k_r = 100$, $k_c = 100$ and the desired trajectory of the leader robot R_4 is given by $\mathbf{z}_d = [72\cos t, 84 + 72\sin t]^\top$ in millimeters. The robots converge to the desired formation pattern, which is observed by the robots' trajectories in Fig. 7a and the errors' convergence shown in Fig. 7b. Note that the errors of the real robots are smaller than the errors of the virtual robots in the experimental data. The control inputs are depicted in Fig. 7c. Note that the control performance is affected by the resolution of the camera, the sample time and the non-modeled dynamics presented by the floor friction and other real effects.

6. CONCLUSIONS

This paper addresses the modeling, control and experimentation of cyber-physical formations for mobile single integrator 2D robots over two workspaces. The control strategy employs virtual agents that converge to the physical robots moving in the opposite workspace. Convergence is guaranteed for a general case of n robots and the robots behave as if they moved in a single workspace. The proposed approach can be used for a family of nonholonomic mobile robots that can be reduced to single 2D integrators by an appropriate feedback linearization. The control strategy was validated through numerical simulations. In addition, an innovative low-cost experimental platform was built, where an experiment was run using four unicycle robots in two different physical workspaces with internet communication. Further work will address other robot dynamics and delays and intermittence effects due to the internet communication.

REFERENCES

Canudas de Wit, C., Siciliano, B., and Bastin, G. (eds.) (1996). *Theory of Robot Control*. Springer London.

Escobar, L., Moyano, C., Aguirre, G., Guerra, G., Allauca, L., and Loza, D. (2020). Multi-robot platform with features of cyber-physical systems for education applications. In *2020 IEEE ANDESCON*, 1–6.

Farrugia, J.L. and Fabri, S.G. (2018). Swarm robotics for object transportation. In *2018 UKACC 12th International Conference on Control (CONTROL)*, 353–358.

Ferreira-Vazquez, E.D., Hernández-Martínez, E.G., Flores-Godoy, J.J., Fernandez-Anaya, G., and Paniagua-Contro, P. (2016). Distance-based formation control using angular information between robots.

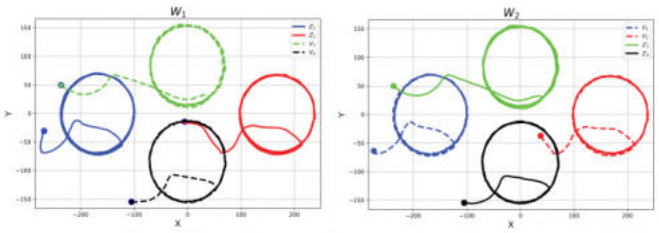

(a) Trajectories of robots.

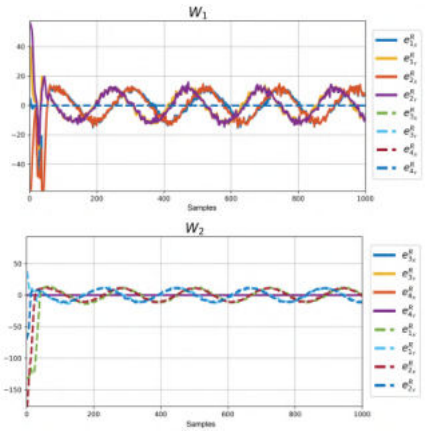

(b) Convergence of the errors.

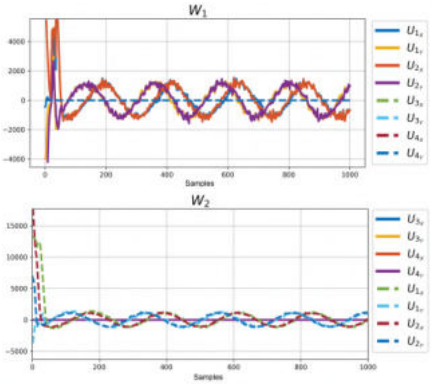

(c) Control inputs.

Fig. 7. Experimental work.

Journal of Intelligent & Robotic Systems, 83(3), 543–560.

Gallo, T., Cagnetti, C., Silvestri, C., and Ruggieri, A. (2021). Industry 4.0 tools in lean production: A systematic literature review. *Procedia Computer Science*, 180, 394–403. Proceedings of the 2nd International Conference on Industry 4.0 and Smart Manufacturing (ISM 2020).

González-Sierra, J., Aranda-Bricaire, E., and Hernandez-Martinez, E.G. (2013). Formation tracking with orientation convergence for groups of unicycles. *International Journal of Advanced Robotic Systems*, 10(3), 180.

Hernandez-Martinez, E.G., Foyo-Valdes, S.A., Puga-Velazquez, E.S., and Meda-Campaña, J.A. (2014). Hybrid architecture for coordination of agvs in fms. *Int. Journal of Advanced Robotic Systems*, 11(3), 41.

Hernandez-Martinez, E.G., Flores-Godoy, J.J., and Fernandez-Anaya, G. (2013). Decentralized discrete-time formation control for multirobot systems. *Discrete Dynamics in Nature and Society*, 2013, 746713.

Kim, K.J., Suh, I.H., Kim, S.H., and Oh, S.R. (2008). A novel real-time control architecture for internet-based thin-client robot; simulacrum-based approach. In *2008 IEEE International Conference on Robotics and Automation*, 4080–4085.

Kruglova, T., Schmelev, I., Sushkov, I., and Filatov, R. (2019). Cyber-physical system of the mobile robot's optimal trajectory planning with taking into account electric motors deterioration. In *2019 International Multi-Conference on Industrial Engineering and Modern Technologies (FarEastCon)*, 1–5.

Lian, Y., Xie, W., Yang, Q., Zhang, L., Lin, D., and Zhou, Y. (2021). A novel multi-warehouse mobile robot hierarchical scheduling strategy based on industrial cyber-physical system. In *2021 4th IEEE International Conference on Industrial Cyber-Physical Systems (ICPS)*, 263–269.

Lo, W.T., Liu, Y.H., Elhajj, I., Xi, N., Shi, Y., and Wang, Y. (2003). Co-operative control of internet based multi-robot systems with force reflection. In *2003 IEEE International Conference on Robotics and Automation (Cat. No.03CH37422)*, volume 3, 4414–4419.

Lopez-Gonzalez, A., Ferreira, E., Hernández-Martínez, E.G., Flores-Godoy, J.J., Fernandez-Anaya, G., and Paniagua-Contro, P. (2016). Multi-robot formation control using distance and orientation. *Advanced Robotics*, 30(14), 901–913.

Mantha, B.R., Jung, M.K., García de Soto, B., Menassa, C.C., and Kamat, V.R. (2020). Generalized task allocation and route planning for robots with multiple depots in indoor building environments. *Automation in Construction*, 119, 103359.

Oh, K.K., Park, M.C., and Ahn, H.S. (2015). A survey of multi-agent formation control. *Automatica*, 53, 424–440.

Olfati-Saber, R. (2007). Design of behavior of swarms: From flocking to data fusion using microfilter networks. In *Cooperative Control of Distributed Multi-Agent Systems*, 19–41. John Wiley & Sons, Ltd.

Pikner, H., Sell, R., Karjust, K., Malayjerdi, E., and Velsker, T. (2021). Cyber-physical control system for autonomous logistic robot. In *2021 IEEE 19th International Power Electronics and Motion Control Conference (PEMC)*, 699–704.

Shahzad, A. and Roth, H. (2016). Bilateral telecontrol of automerlin mobile robot with fix communication delay. In *2016 IEEE International Conference on Automation, Quality and Testing, Robotics (AQTR)*, 1–6.

Valentim, T., Cunha, R., Oliveira, P., Cabecinhas, D., and Silvestre, C. (2019). Multi-vehicle cooperative control for load transportation. *IFAC-PapersOnLine*, 52(12), 358–363. 21st IFAC Symposium on Automatic Control in Aerospace ACA 2019.